Journal of Molecular Liquids 456 (2026) 129603

Contents lists available at ScienceDirect

Journal of Molecular Liquids

journal homepage: www.elsevier.com/locate/molliq

Thermophysical characterization of substances used as flavorings

Roberto Martín-Ramo [a], Candela Romero [a], José Muñoz-Embid [a,b], Héctor Artigas [a,b], Carlos Lafuente [a,b], Manuela Artal [a,b,*]

[a] Departamento de Química Física, Facultad de Ciencias, Universidad de Zaragoza, Zaragoza, Spain
[b] Instituto Agroalimentario de Aragón - IA2 (Universidad de Zaragoza - CITA), Zaragoza, Spain

ARTICLE INFO

Keywords:
Essential oil
Terpenes
Anisyl alcohol
Thermodynamic properties
Viscosity
PC-SAFT EoS

ABSTRACT

Essential oils possess numerous health benefits. Their components, often terpene and aromatic compounds, are characterized by a distinctive aroma and flavor. Consequently, they are widely used in the food, cosmetic, and pharmaceutical industries. However, their comprehensive thermophysical characterization is still lacking, which is fundamental for the optimal operational design of the processes in which they are used. In this work, the density, speed of sound, refractive index, isobaric molar heat capacity, surface tension, and viscosity of five flavorings were determined and discussed. The studied substances were anisyl alcohol, linalool, β-citronellol, citronellal, and eucalyptol. Except for the first one, the others exhibited densities lower than that of water. Anisyl alcohol was also the most compact and viscous compound. The results were explained based on the structure (number of donor and acceptor sites and geometry) of the compounds. Furthermore, the PC-SAFT parameters of the pure compounds were obtained to predict their thermodynamic behavior under any experimental conditions. The deviations in the modeling of density and isobaric molar heat capacity were less than 1.1% and 4.1%, respectively.

1. Introduction

The search for a suitable solvent, both in terms of its effectiveness and sustainability, is one of its fundamental principles within green chemistry [1]. Regarding the first, every industrial process must be optimized regardless of its nature (solubilization, extraction, among others). To this end, the use of computer tools has become widespread, frequently employing thermodynamic models of group contributions, equations of state, and semi-empirical equations. Their development and validation in all cases require reliable thermophysical property values for the pure compounds involved. Determining phase change, volumetric, acoustic, surface, and transport properties allows for an understanding of the cohesive forces within the fluid. It also allows the acquisition of the necessary parameters to predict the values of these properties, or others derived from them, under a wide range of conditions, including their extension to mixtures where they are present. Furthermore, sustainability implies the replacement of traditional solvents with more eco-friendly ones. From an economic standpoint, the change should preferably be made using fluids with similar thermophysical behavior to avoid facilities modifications. Various organizations have developed software programs that facilitate this search using extensive databases. For instance, in the sustainable solvents selection and substitution software (SUSSOL) [2], each solvent is described by 22 thermophysical properties and including the melting point, density, refractive index, surface tension, and viscosity. In the solvent selection tool developed by AstraZeneca [3] the isobaric molar heat capacity is also included in its database. All of the above reflects the interest in studying the thermophysical behavior of both pure compounds and mixtures, in the implementation of sustainable processes. Nevertheless, there are liquids such as some key components of essential oils (EOs) that have barely been characterized. Throughout history, many civilizations have incorporated the use of EoS into their culture, religious practices, cosmetics, and medicine [4]. They are defined as aromatic volatile liquids derived from natural plants. Each one is a mixture of a variety of substances, among which aromatic compounds, terpenes, and their derivatives stand out [5–7].

In this work, we present data of five thermodynamic and one transport properties for five flavoring agents. They have been recognized Food and Drug Administration (FDA) as safe compounds for consumption and the Flavor and Extract Manufactures Association (FEMA) has assigned them a number that identifies them as GRAS. Anisyl alcohol (FEMA 2099) is a common compound in the manufacture

* Corresponding author at: Departamento de Química Física, Facultad de Ciencias, Universidad de Zaragoza, Zaragoza, Spain
E-mail address: martal@unizar.es (M. Artal).

https://doi.org/10.1016/j.molliq.2026.129603
Received 25 February 2026; Received in revised form 20 April 2026; Accepted 21 April 2026
Available online 25 April 2026

of personal care products, acting as a dermatological moisturizer. It provides a sweet floral aroma, making it a valuable food flavoring. Furthermore, the presence of the methoxy group in its structure makes it a good reaction intermediate in fine chemistry. It is generally obtained from petrochemical derivatives for economic reasons, although biosynthetic pathways using microorganisms are being evaluated [8,9]. Linalool (FEMA 2635) is an acyclic monoterpene alcohol obtained by fractional distillation of natural sources such as cinnamon, coriander, and lavender. Its consumption is widespread in the cosmetic and agri-food industry as a flavoring and fragrance due to its floral scent. It also has a significant effect on the central nervous system thanks to its neurotransmitter-modulating properties, and antibacterial properties [10,11]. Citronellol (FEMA 2309) and citronellal (FEMA 2307) are two monoterpenes of great interest in the field of biotechnology. The former is an alcohol, and the latter, an aldehyde. Both are found in the essential oils of plants of the genus Cymbopogon and can be isolated by steam distillation, solvent extraction, and ultrasound techniques. They are used in the preparation of cosmetics and fragrances, possessing antibacterial, antifungal, and repellent properties. A wide variety of pharmacological activities have also been described. Among others, they are anticonvulsant, anti-inflammatory, and antinociceptive, and have demonstrated benefits in the glutamatergic system responsible for chronic pain [12–15]. Eucalyptol (FEMA 2465) is a cyclic monoterpene, the major component of eucalyptus oil, and is obtained from it by steam distillation or solvent extraction using assisted techniques. Its spicy, minty, and fresh aroma makes it a pleasant additive for food and cosmetics. In pharmacology, its activity against cancer, diabetes, hypertension, infectious and neurological diseases, and respiratory and gastrointestinal disorders has been reported. Its ability to improve drug permeability through the dermis is also well known. Furthermore, it has been used as a sustainable solvent in organic catalytic reactions [16,17]. Despite the widespread use of these compounds, a comprehensive study of their thermophysical behavior is missing. Values of density and speed of sound of anisyl alcohol at three temperatures were found [18]. Several papers report data of vapor pressures, density, refractive index, and viscosity of linalool [19–24]. A single density value at 293.15 K was found for citronellol [25,26]. The eucalyptol is the most studied compound of those characterized here. Several authors published data of density, isobaric molar heat capacity, and viscosity [26–33]. No data were found for citronellal. Finally, surface tension values have not been published for any of these compounds either.

This work focuses on the determination and discussion of several thermodynamic and transport properties of different organic compounds widely used as additives for their fragrant and flavoring characteristics. The paper is organized as follows. First, the chemicals studied are reported, as well as the main characteristics of the experimental devices used. The following section contains a brief description of the PC-SAFT EoS, and the equations used for calculating the derived properties and the correlations. Later, the experimental and calculated property values are presented and compared with available literature data. A specific section is included in which thermophysical properties are related to the structure of compounds. The last section includes the estimation of the parameters necessary for modeling the thermodynamic behavior of these compounds with PC-SAFT and its results.

2. Materials and methods

2.1. Chemicals

The characteristics and the structures of the compounds studied are listed in Table 1 and Fig. 1, respectively. They were provided by Sigma-Aldrich and used as supplied. The water content measured by the Karl-Fischer method was less than 350 ppm for all compounds.

Table 1
Characteristics of the compounds.[a]

Compound (Acronym)	IUPAC name	CAS no	Purity[a]	M/(g/mol)
Anisyl alcohol (Aa)	(4-Methoxyphenyl) methanol	105–13-5	99.3%	138.17
Linalool (L)	2,6-Dimethyl-2,7-octadien-6-ol	78–70-6	99.0%	154.25
β-Citronellol (Co)	3,7-Dimethyloct-6-en-1-ol	106–22-9	97.1%	156.27
Citronellal (Ca)	3,7-Dimethyloct-6-en-1-al	106–23-0	98.5%	154.25
Eucalyptol (E)	1,3,3-trimethyl-2-oxabicyclo[2.2.2]octane	470–82-6	99.7%	154.25

[a] According to the certificate of analysis (COA) of the batch provided by the manufacturer

2.2. Thermal properties

A differential scanning calorimeter (TA Instruments DSC Q2000) with an RCS cooling system was used to determine properties of phase change as melting temperature (T_m), and melting enthalpy (ΔH_m). A standard of Indium was used to calibrate the temperatures and heat flow and the uncertainties estimated were $u(T)$=0.5 K and $u(\Delta H)$=1 kJ/mol. For each sample, an Aluminum disc was filled with a mass between 8 and 14 mg of compound. Later, it was cooled to 213 K at 3 K/min and subsequently heated at the same scan rate to 313 K. The tabulated data correspond to the maximum of the peak. The same device with the same samples was used to determine the isobaric molar heat capacity ($C_{p,m}$) over the working temperature range. Here, synthetic sapphire was used as the recommended standard material. The combined uncertainty (k=2, 0.95 level of confidence) calculated by comparison with accepted values over the temperature range 262–343 K, was $U_c(C_{p,m})$=1%.

2.3. Thermophysical properties

The measurement of the rest of the thermophysical properties was performed with apparatus widely described in the literature. The density (ρ) and speed of sound (u) were determined by Anton Paar DSA 5000 densimeter and sound analyzer operating to 3 MHz. The device was calibrated with dry air and water MilliQ as reference fluids. The thermostat control was performed with a Peltier device. The refractive index (n_D) was measured at the wavelength of the sodium D line (589.3 nm) using an Abbemat-HP Dr. Kernchen refractometer calibrated with MilliQ water. Again, a Peltier system controlled the temperature of the sample. The surface tension (γ) was determined with a Lauda TVT-2 tensiometer which includes a Lauda E-200 thermostat. The calibration was performed with water MilliQ. Each value was the result of averaging 6 cycles of 6 drops per cycle. Finally, kinematic viscosity (ν) was determined using an Ubbelohde capillary viscometer (k= 0.1007, and 0.02981 mm^2/s^2) and the measurements were taken with a Schott-Geräte AVS-440 automatic measurement unit. The temperature was controlled with a Schott-Geräte CT 1150/2 thermostat. Table 2 reports a summary with the characteristics of each experimental setup. All them were checked with benzene and cyclohexane as standard fluids [34,35]. The comparison between our data and those from the literature data is given in Table 2 as mean relative deviations ($MRD(Y)$). For all properties, each tabulated value was calculated as the average of two replicates in which the coefficient of variation was lower than the experimental uncertainty. Details regarding the calculation of uncertainties are included in the Supplementary File.

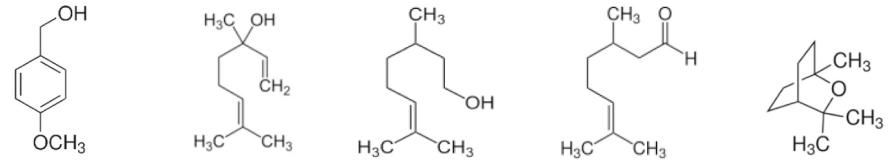

Anisyl alcohol Linalool β-Citronellol Citronellal Eucalyptol

Fig. 1. Structures of the compounds studied.

Table 2
Overview of the different apparatus utilized to measure several properties.

Property	Devices	$u(T)$/K	$U_c(Y)^a$	$MRD(Y)^b$/%
Density, ρ	Oscillating U-tube density meter, Anton Paar DSA 5000	0.005	0.1 kg/m^3	0.004
Speed of sound, u	Sing-around technique in a fixed-path interferometer, Anton Paar DSA 5000	0.005	0.8 m/s	0.026
Refractive index, n_D	Standard Abbe refractometer, Abbemat-HP refractometer Dr. Kernchen	0.01	$2{\cdot}10^{-5}$	0.007
Surface tension, γ	Drop volume tensiometer, Lauda TVT-2	0.01	1%	0.21
Kinematic viscosity, ν	Capillary viscosimeter Ubbelohde, Schoot-Geräte AVS-440	0.01	1%	0.28

$^a k = 2$ (0.95 level of confidence); $^b MRD(Y) = \frac{100}{n}\sum_{i=1}^{n}\left|\frac{Y_{i,lit} - Y_{i,exp}}{Y_{i,exp}}\right|$

3. Theory and calculations

3.1. PC-SAFT EoS

A comprehensive description of this equation of state can be found in the literature [36,37]. Here, we will give a brief summary. The Helmholtz energy ($\tilde{a}$) is described as the sum of an ideal gas contribution ($\tilde{a}^{id}$) and a residual one ($\tilde{a}^{res}$). The last one contains a repulsive term used by the hard-chain reference system ($\tilde{a}^{hc}$), and various attractive contributions as the dispersive ($\tilde{a}^{dis}$) and association ($\tilde{a}^{assoc}$) terms. The equations are:

$$\tilde{a}^{res} = \tilde{a}^{hc} + \tilde{a}^{dis} + \tilde{a}^{assoc} \tag{1}$$

$$\tilde{a}^{hc} = m\tilde{a}^{hs} - (m-1)\ln g^{hs} \tag{2}$$

$$\tilde{a}^{dis} = -2\pi\rho m^2\left(\frac{\varepsilon}{kT}\right)\sigma^3\sum_{i=0}^{6}\left[a_{0i} + \frac{m-1}{m}a_{1i} + \frac{m-1}{m}\frac{m-2}{m}a_{2i}\right]\eta^i - \pi\rho mkT\left(\frac{\partial\rho}{\partial p}\right)_{hc} m^2\left(\frac{\varepsilon}{kT}\right)^2\sigma^3\sum_{i=0}^{6}\left[b_{0i} + \frac{m-1}{m}b_{1i} + \frac{m-1}{m}\frac{m-2}{m}b_{2i}\right]\eta^i \tag{3}$$

$$\tilde{a}^{assoc} = \sum_A\left[\ln\left(1+\rho X^A\Delta\right)^{-1} - \frac{\left(1+\rho X^A\Delta\right)^{-1}}{2}\right] + \frac{1}{2}S \tag{4}$$

$$\Delta = \kappa^{A_iB_i}\sigma^3 g^{hs}\left[\exp\left(\frac{\varepsilon^{A_iB_i}}{kT}\right) - 1\right] \tag{5}$$

where m is the chain segment number, g^{hs} is the radial pair distribution function of the segments, $\tilde{a}^{hs}$ is the Helmholtz energy of the hard sphere, ρ is the density, p is the pressure, T is the temperature, σ is the segment diameter, ε is the segment energy, η is the packing fraction, X^A is the fraction of unbonded monomers, Δ is the tendency to form n-mers, $\kappa^{A_iB_i}$ is the association volume, $\varepsilon^{A_iB_i}$ is the association energy, and S is the number of associated sites of the compound. The thermodynamic properties of n-alkanes were used to obtain the values of the *universal constants* ($a_{0i}, a_{1i}, a_{2i}, b_{0i}, b_{1i}$, and b_{2i}). From all this, five parameters and an association scheme are needed to characterize each pure substance. Three of them are geometric parameters (m, σ and ε) and two are association parameters ($\kappa^{A_iB_i}$ and $\varepsilon^{A_iB_i}$). Typically, they are obtained by fitting the vapor pressures and density data of the compound.

3.2. Estimation of the derived properties

From the experimental data of the density (ρ), speed of sound (u), refractive index (n_D), isobaric molar heat capacity ($C_{p,m}$), surface tension (γ), and dynamic viscosity (η), different derived properties can be obtained. They are the isobaric expansibility (α_p), isentropic compressibility (κ_S), free intermolecular length (L_f), molar volume (V_m), molar refraction (R_m), polarizability (α), free volume (f_m), Joule-Thomson coefficient (μ_{JT}), entropy (ΔS_S) and enthalpy (ΔH_S) of surface, and activation energy of viscous flow ($E_{a,\eta}$). The corresponding equations are the following:

$$\alpha_p = -\frac{1}{\rho}\left(\frac{\partial\rho}{\partial T}\right)_p \tag{6}$$

$$\kappa_S = \frac{1}{\rho u^2} \tag{7}$$

$$L_f = K\sqrt{\kappa_S} \tag{8}$$

$$V_m = \frac{M}{\rho} \tag{9}$$

$$R_m = V_m\frac{\left(n_D^2-1\right)}{\left(n_D^2+2\right)} = N_A\frac{4\pi}{3}\alpha \tag{10}$$

$$\%f_m = \frac{\left(V_m - R_m\right)}{V_m} \tag{11}$$

$$\mu_{JT} = \frac{V_m}{C_{p,m}}\left(T\alpha_p - 1\right) \tag{12}$$

$$\Delta S_s = -\left(\frac{\partial\gamma}{\partial T}\right)_p \tag{13}$$

$$\Delta H_S = \gamma - T\left(\frac{\partial\gamma}{\partial T}\right)_p \tag{14}$$

$$E_{a,\eta} = R\frac{\partial(\ln\eta)}{\partial\left(\frac{1}{T}\right)} \tag{15}$$

Where p and T are the pressure, and temperature, respectively, R is the gas constant, N_A is the Avogadro number, and K=(91.368 + 0.3565T)10^{-8} is the constant of Jacobson [38].

3.3. Estimation of the critical temperature

The critical temperature of the fluids can be calculated from equations of state such as PC-SAFT (section 3.1), group contribution methods such as the one developed by Joback [39], and correlations such as the equations of Guggenheim [40] and Eötvos [41]. The last two equations are based in the principle of the corresponding states, and are in agreement with the fact that γ=0 at the critical point, where the meniscus of the interface disappears. The expressions are:

$$\gamma = \gamma_0(1 - T/T_c)^{11/9} \tag{16}$$

$$\gamma(M/\rho)^{2/3} = K(T_c - T) \tag{17}$$

Where γ_0 is the surface tension at 0 K, M is the molar mass of the liquid, and γ and ρ are the surface tension and density at the temperature T. The difference between the two equations lies in the shape of the proposed $\gamma - T$ curve. Guggenheim proposed a power-law relationship (eq. 16), while Eötvös proposed a linear one (eq. 17), making the former more accurate in the region near the critical point. Furthermore, the latter requires data on γ and ρ under the same conditions of p and T.

3.4. Estimation of the surface tension

Surface tension results from the asymmetry of intermolecular forces at the interface. When a molecule moves from the interior of the fluid, where intermolecular forces are similar in all directions, to the surface where this symmetry is broken, the molecule will become polarized. Therefore, a correlation can be established between γ and n_D. Note that this correlation does not hold true for liquids capable of forming strong hydrogen bonds. The proposed equation by Papazian [42] is:

$$\gamma = A\left(\frac{n_D^2 - 1}{2n_D^2 + 1}\right) + B \tag{18}$$

Furthermore, several authors have proposed correlations between gamma and net, since both properties reflect intermolecular interactions, although they represent different phenomena. The empirical equations proposed by Pelofsky and Murkerjee [43] are:

$$\ln\gamma = \ln A_1 + \frac{B_1}{\eta} \tag{19}$$

$$\ln\gamma = \ln A_2 + \frac{B_2}{3}\ln\eta \tag{20}$$

Where A, B, A_1, A_2, B_1, and B_2 are the fit coefficients. The coefficient A_1 would correspond to the γ at the nucleation temperature, where the reciprocal viscosity tends to zero ($\eta^{-1} \rightarrow 0$). The coefficient B_1 would be related to the intermolecular potential energy.

4. Results and discussion

4.1. Phase change

The thermograms of all compounds characterized are reported in Fig. S1. Fig. 2 displays the results for anisyl alcohol and eucalyptol, which are the only compounds that showed thermal events in the studied temperature range. For both, the values of the properties of phase change including melting and crystallization processes are listed in Table 3. The melting temperatures (T_m) found in the literature [44,45], and the melting enthalpies (ΔH_m) estimated using the Joback method [39] are also reported in this table. An excellent agreement was found.

4.2. Thermophysical properties

The thermophysical properties of a solvent determine the operational design of industrial processes and their effectiveness. Here, results of six of them in a temperature range, in intervals of 2.5 K, are presented and discussed. They were the density (ρ), speed of sound (u), refractive index (n_D), isobaric molar heat capacity ($C_{p,m}$), surface tension (γ), and dynamic viscosity (η). The lowest working temperature depended on the melting point of the compounds and operational limitations of the facilities. For Aa, measurements were taken starting at 298.15 K. For the rest, the initial temperature was 278.15 K, except for the refractive index, because the refractometer operates from 283.15 K. The highest temperature was in all cases of 338.15 K. The values of all properties at each temperature are reported in the supplementary file (Tables S1-S5). In addition, Table 4 lists the experimental and calculated property data at 298.15 K to make it easier to follow the discussion. As is usual in

Table 3
Properties of phase change of anisyl alcohol and eucalyptol. Melting (T_m), and crystallization (T_{cr}) temperatures, and melting (ΔH_m), and crystallization (ΔH_{cr}) enthalpies.

Compounds	T_m/K	ΔH_m/(kJ/mol)	T_{cr}/K	ΔH_{cr}/(kJ/mol)
Anisyl alcohol	296.60 [a] (297.15–298.15) [b]	13.3/15.4 [c]	280.92	14.1
Eucalyptol	273.32 [a]/274.63 [d]	11.1/10.2 [c]	233.41	10.4

[a]This work; [b] [45]; [c]Joback method; [d][44].

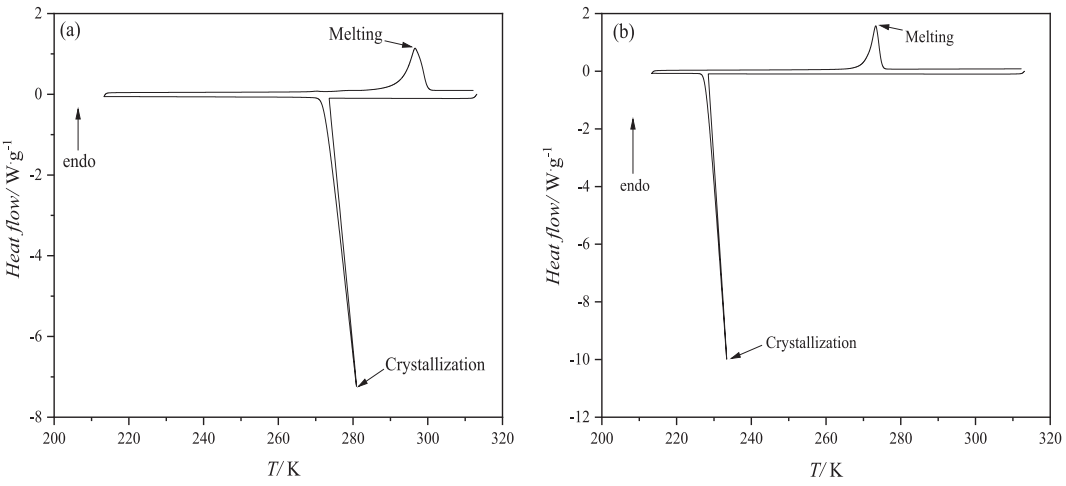

Fig. 2. DSC thermograms of (a) anisyl alcohol and (b) eucalyptol.

Table 4
Thermophysical properties[a] of the compounds studied at $T = 298.15$ K and $p = 0.1$ MPa. Density (ρ), speed of sound (u), refractive index (n_D), isobaric molar heat capacity ($C_{p,m}$), surface tension (γ), dynamic viscosity (η), Isobaric expansibility (α_p), isentropic compressibility (κ_S), free intermolecular length (L_f), molar refraction (R_m), polarizability (α), free volume (f_m), Joule-Thomson coefficient (μ_{JT}), entropy (ΔS_S) and enthalpy (ΔH_S) of surface, and activation energy of viscous flow ($E_{a,\eta}$).

Property	Anisyl alcohol	Linalool	β-Citronellol	Citronellal	Eucalyptol
ρ/(kg/m^3)	1108.02	859.68	851.62	846.21	920.37
u/(m/s)	1604.59	1314.70	1375.63	1332.63	1281.48
n_D	1.5435	1.45949	1.45459	1.44299	1.45543
$C_{p,m}$/(J/mol·K)	290	388	370	321	272
γ/(mN/m)	43.21	26.75	28.13	27.94	27.75
η/(mPa·s)	14.743	4.563	9.003	1.435	2.570
α_p/(kK^{-1})	0.496	0.988	0.833	0.957	0.939
κ_s/ (TPa^{-1})	350.33	672.99	620.51	665.43	661.63
L_f/Å	0.370	0.513	0.492	0.510	0.508
R_m/ (cm^3/mol)	39.336	49.061	49.747	48.324	45.509
α/Å^3	15.59	19.45	19.72	19.15	18.04
f_m/ (cm^3/mol)	85.36	130.33	133.75	133.96	122.09
%f_m	68.46	72.64	72.89	73.49	72.85
μ_{JT}/ (K/MPa)	−0.341	−0.327	−0.373	−0.407	−0.444
ΔS_S/(mN/m·K)	0.113	0.0938	0.0868	0.108	0.104
ΔH_S/(mN/m)	76.84	54.72	54.01	60.20	58.77
$E_{a,\eta}$/(kJ/mol)	34.76	31.02	28.72	13.27	16.61

[a] Standard uncertainties are: $u(T)$=0.005 K for density and speed of sound and 0.01 K for the rest of properties; $u(p)$=0.5 kPa. The combined expanded uncertainties (0.95 level of confidence, k=2) are $U_c(\rho)$=0.1 kg/m^3; $U_c(u)$=0.8 m/s; $U_c(n_D)$=2·10^{-5}; $U_c(C_{p,m})$=1%; $U_c(\gamma)$=1%; $U_c(\eta)$=1%; $U_c(\alpha_p)$=0.09 kK^{-1}; $U_c(\kappa_s)$=0.22 TPa^{-1}; $U_c(R_m)$=0.004 cm^3/mol; $U_c(f_m)$=0.03 cm^3/mol; $U_c(\mu_{JT})$=1%; $U_c(\Delta S_S)$=0.001 mN/m·K; $U_c(\Delta H_S)$=0.06 mN/m.

liquid systems, a linear equation was used to correlate the experimental thermodynamic properties with the temperature. The coefficients are summarized in Table 5.

4.2.1. Density

The density order for the studied compounds was Aa>E > L > Co > Ca. The difference between the density of a liquid i and that of water (ρ_i-ρ_w) is an important factor in the possible applications of a solvent. Except for Aa, the density of the compounds studied was lower than that of water and the difference was greater than 80 kg/m^3 in all cases. This fact allows to ensure a good phase separation in liquid-liquid equilibrium processes. Several data were found in the literature for Aa [18], L [19–22], and E [27–30], and our values matched very well with them. The mean relative deviations were 0.08% for Aa, lower than 0.34% for L, and lower than 0.18% for E. A graphical comparison is reported in Fig. S2a-S4a. For Co, only one data point was found [25] and it was only 0.2 kg/m^3 higher than ours. The increase in energy in the system due to the temperature increase increases the mobility of the molecules, weakening the interactions between them. Consequently, the density decreases (Fig. 3a), and the variation in liquids is usually linear (Table 5). A quantification of the influence of T on ρ was performed by calculating the isobaric expansivity (α_p) with the eq. 2. The value obtained for Aa was almost half that of the other substances (Table 4), consistent with its considerably higher ρ (up to 30%). The α_p increased slightly with T (Fig. 4a), and the values of the temperature coefficient ($\partial\alpha_p/\partial T$) in the T studied range were (2.51 ± 0.01)·10^{-4} kK^{-2} for Aa, (7.04 ± 0.02)·10^{-4} kK^{-2} for Co, and a mean of (9.4 ± 0.5)·10^{-4} kK^{-2} for the rest.

Table 5
Correlation of each thermodynamical property with temperature [a] of the fluids studied [b]. Fitting parameters (A_Y,B_Y) and regression coefficients (R^2).

Property	Fluid	A_Y	B_Y	R^2
Density, ρ /(kg/m^3)	Aa	1272.02	−0.550	0.9999
	L	1113.01	−0.849	0.9999
	Co	1063.21	−0.709	0.9999
	Ca	1087.60	−0.810	0.9999
	E	1177.92	−0.864	1.0000
Speed of sound, u /(m/s)	Aa	2434.5	−2.784	0.9998
	L	2437.0	−3.765	0.9999
	Co	2465.9	−3.657	0.9998
	Ca	2483.4	−3.861	0.9998
	E	2438.0	−3.875	0.9995
Refractive index, n_D	Aa	1.6634	−4.0·10^{-4}	0.9962
	L	1.60397	−4.8·10^{-4}	1.0000
	Co	1.57390	−4.0·10^{-4}	0.9997
	Ca	1.59127	−5.0·10^{-4}	0.9994
	E	1.59281	−4.6·10^{-4}	1.0000
Isobaric molar heat capacity, $C_{p,m}$/(J/mol·K)	Aa	106.76	0.6152	0.9999
	L	164.13	0.7505	1.0000
	Co	31.278	1.1355	0.9998
	Ca	178.37	0.4799	0.9999
	E	91.09	0.6052	0.9999
Surface tension, γ/(mN/m)	Aa	76.87	−0.1128	0.9992
	L	54.67	−0.0938	0.9995
	Co	54.03	−0.0868	0.9997
	Ca	60.22	−0.1082	0.9997
	E	58.77	−0.104	0.99877

[a] $Y = A_Y + B_Y T$; [b] Aa, anysil alcohol; L, linalool; Co, β-citronellol; Ca, citronellal; E, eucalyptol.

4.2.2. Speed of sound

The more compact a material, the faster the speed of sound. The values determined for Aa were much higher than for the other compounds. On average, sound propagated 298 m/s faster in Aa than the rest. This fact was consistent with the presence of greater intermolecular interaction in the methoxyl alcohol. Compaction is prevented by increasing the thermal energy of the system, so the slope of the $u - T$ correlation was negative (Fig. 3b, Table 5). Shakila et al. [18] published sound speeds of Aa at three temperatures. The mean relative deviation from our values was 0.08% (Fig. S2b). No further bibliographic data were found. As a consequence of the larger ρ and u values, the compressibility under isentropic conditions (κ_S, eq. 7) and the intermolecular distance (L_f, eq. 8) were much lower as shown in Table 4 and Fig. 4b and c. From the figures, it can be seen that the influence of T on the derived acoustic properties entailed positive temperature coefficients. For L_f, these values were (1.51 ± 0.01)·10^{-3} Å·K^{-1} for Aa, (2.56 ± 0.02)·10^{-3} Å·K^{-1} for Co, and a mean of (2.85 ± 0.03)·10^{-3} Å·K^{-1} for the rest.

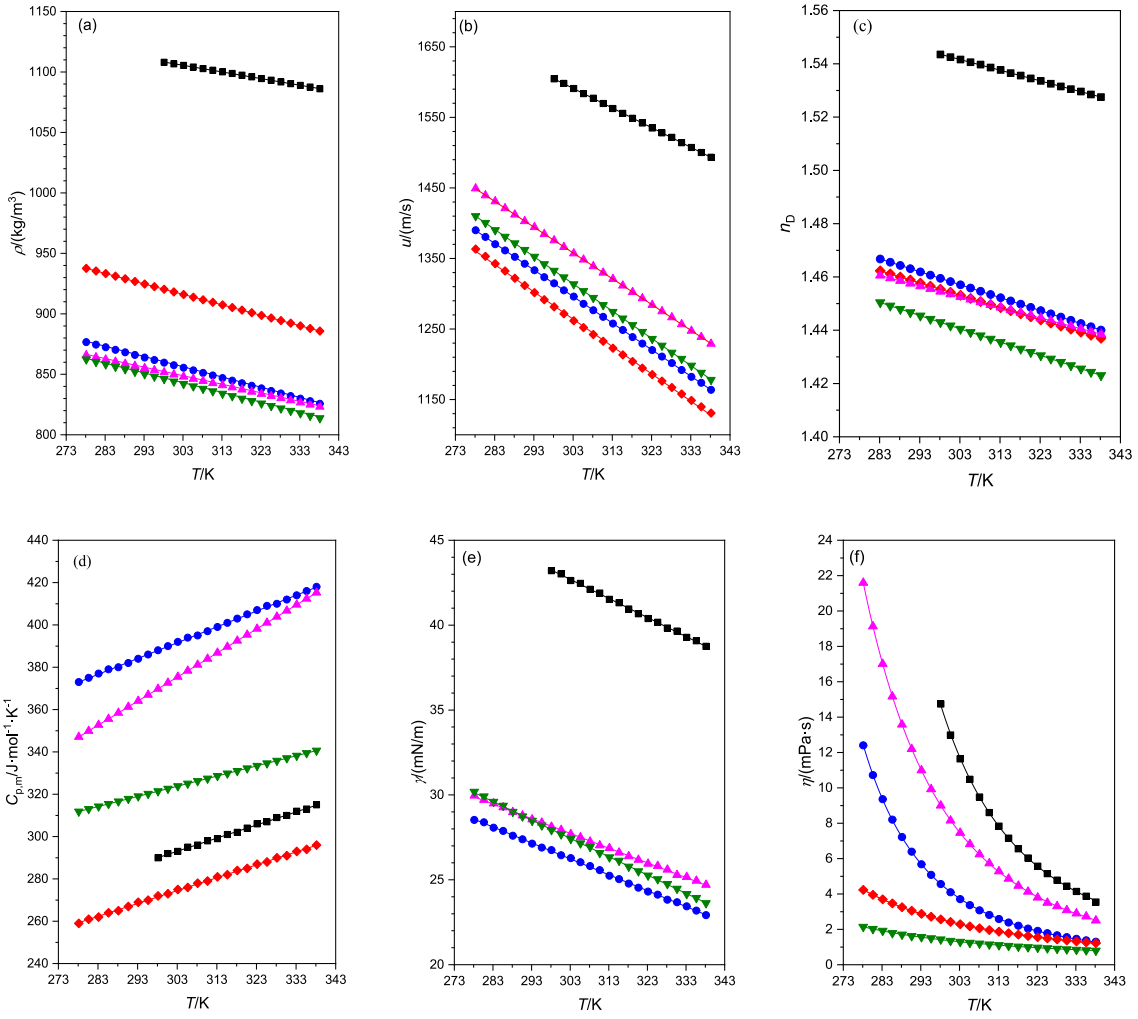

Fig. 3. Experimental thermophysical properties of the fluids studied at p=0.1 MPa, and at several temperatures (T). (a) Density (ρ); (b) speed of sound (u); (c) refractive index (n_D); (d) isobaric molar heat capacity ($C_{p,m}$); (e) surface tension (γ); and (f) dynamic viscosity (η). (■), Anisyl alcohol; (●), Linalool; (▲), β-citronellol; (▼), citronellal; (◆), eucalyptol. Points, experimental values; lines, correlated data.

4.2.3. *Refractive index*

Contrary to what happens with sound, light travels faster in less compact media. Considering that the n_D is defined as the ratio between the speed of light in the vacuum and its speed in the medium, the more compact a fluid is, the higher its n_D. As expected after the result of the previous section, Aa had the higher value of this property. The values decreased with T increased due to the thermal motion (Fig. 3c). Table 5 list the coefficients of the linear equation. We can compare bibliographic data with our own for L and Co. In relation to the first, the deviations ($MRD(n_D)$) were 0.02% [19] and 0.04% [21]. Fig. S3b shows the graphical comparison. For the second, the value published for Li et al. [25] was $2.4{\cdot}10^{-4}$ higher than ours. From ρ and n_D data under the same p, T conditions, the molar refraction (R_m) can be calculated (eq. 10). It was practically constant with T for all compounds (Fig. 4d). The values at 298.15 K are listed in Table 4. This property is a measure of the ability of the molecule to distort its electron cloud when subjected to an electric field; that is, it is related to the polarizability (α) (see eq. 10). The α calculated values (Table 4) were in good agreement with those estimated found in the literature [46]: α(Aa) = 14.91 Å^3, α(L) = 18.97 Å^3, α(Co) = 20.05 Å^3, α(Ca) = 19.18 Å^3, and α(E) = 18.54 Å^3. The hard core of a mole of molecules is related to R_m in such a way that the difference between the molar volume and this property is an estimate of the molar free volume (f_m). Table 4 and Fig. 4e report the calculated data, whose increased linearly with T. The sequence obtained for the f_m percentage (eq. 11) was as expected after the results collected in the previous sections (Table 4).

4.2.4. *Isobaric molar heat capacity*

The $C_{p,m}$ is defined as the amount of heat required to raise the temperature of one mole of a substance by one degree. The observed sequence was L > Co > Ca > Aa>E with values between 418 J/mol·K for L at 338.15 K, and 259 J/mol·K for E at 278.15 K. Bibliographic data are available for L, Co and E. For the first one, the value recommended by the NIST database [47] at 293.1 K was 3.02% lower than ours. For Co, our data were higher than those published by Štejfa et al. [26] with a deviation of 3.62%. For E, three datasets were found. Our data were 11.5% lower than those published by Aparicio et al. [28], but agreed with those of Štejfa et al. [48], and Martínez-López et al. [32], with mean deviations of 0.65% in both cases (Fig. S4b). At higher temperatures, a greater number of vibration modes are activated, so the linear $C_{p,m} - T$ correlation has a positive slope (Table 5, Fig. 3d). The temperature change that occurs in a fluid during an expansion process is quantified by the Joule-Thomson coefficient. This parameter can be calculated from $C_{p,m}$ values, and volumetric data at different temperatures (eq. 12). All obtained values were negatives (Table 4) and the estimated temperature coefficients were $(\partial\mu_{JT}/\partial T) = (8.41 \pm 0.07){\cdot}10^{-4}$ MPa^{-1}, $(8.81 \pm 0.04){\cdot}10^{-4}$ MPa^{-1}, $(12.9 \pm 0.12){\cdot}10^{-4}$ MPa^{-1}, $(9.06 \pm 0.04){\cdot}10^{-4}$ MPa^{-1}, and $(12.9 \pm 0.09){\cdot}10^{-4}$ MPa^{-1} for Aa, L, Co,

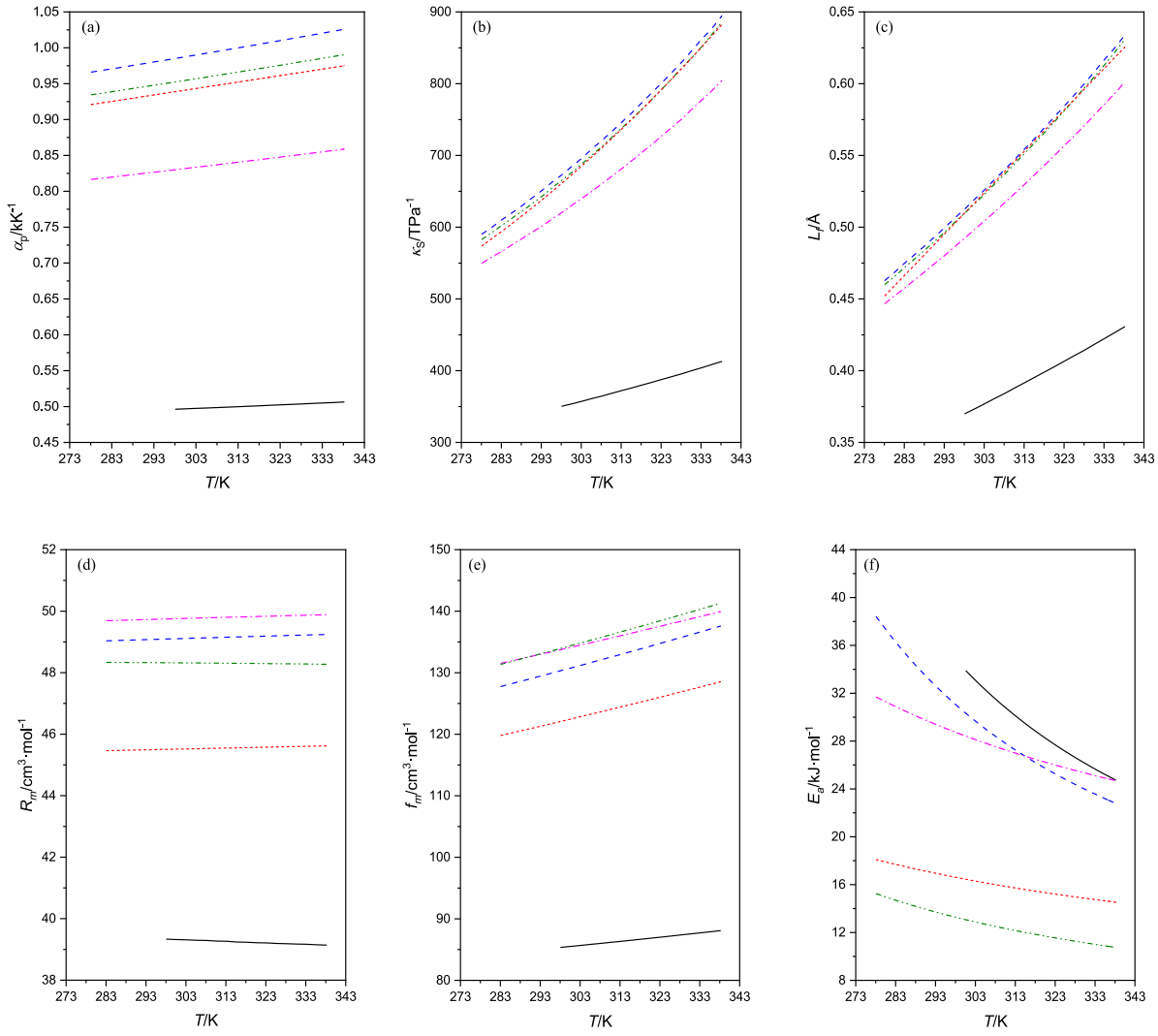

Fig. 4. Calculated thermophysical properties of the fluids studied at p=0.1 MPa, and at several temperatures (T). (a) isobaric expansibility (α_p); (b) isentropic compressibility (κ_S); (c) free intermolecular length (L_f); (d) molar refraction (R_m); (e) free volume (f_m); and (f) activation energy of viscous flow ($E_{a,\eta}$). (—), Anisyl alcohol; (— —), Linalool; (— • —), β-citronellol; (—••—), citronellal; (– – –), eucalyptol.

Ca, and E, respectively.

4.2.5. *Surface tension*

The movement of a molecule towards the surface must overcome cohesive forces so increasing the surface area of a fluid interface involves an energy cost, quantified as surface tension. The higher the γ value, the more structural a fluid is. In this work, most and least structured liquids were Aa and L, respectively, and Co, Ca, and E had similar values. Again, the behavior of the Aa was very different to the rest. Its values ranged from 38.75 to 43.21 mPa·s. For the rest, they were between 22.92 and 30.19 mPa·s. No literature data were found for any of the liquids studied. The decrease in intermolecular forces as the thermal energy of the systems increases causes a decrease in the value of γ. In this work, the decrease was lineal as Fig. 3e shows and Table 5 reports. From the $\gamma - T$ study, entropy and enthalpy of surface can be calculated (eq. 13 and 14) and the values at 298.15 K are listed in Table 4. Small differences in entropy contribution of the different compounds were found. On the other hand, the enthalpy contribution was much higher for Aa due to the presence of stronger intermolecular interactions. Having the values of critical temperature (T_c), and critical pressure (p_c) is essential for calculating other thermodynamic properties and for developing tools that enable the correct design of industrial processes. However, their experimental determination is often costly or even impossible due to the thermal decomposition of the compound. Group contribution models such as the Joback method [39] can estimate these properties. Also, the suppression of the interface at the critical temperature of a substance leads to its surface tension being zero under those conditions. Accordingly, Guggenheim and Eötvös proposed equations (section 3.3) that allow the calculation of T_c from γ and ρ. Considering all models, the T_c predicted with Joback method was the highest for all compounds except for Aa (Table 6). This method typically tends to overestimate the value of the critical properties. A deviation of a 4.55% in T_c and 4.83% in p_c was calculated by comparison with the experimental data of different substances [49]. Comparing Guggenheim and Eötvös equations, the values estimated with the first equation were, on average, a 5.12% higher than those obtained with the second. Moreover, the polarity of a molecule depends on the distribution of forces around it. This distribution changes when a molecule passes to the surface of the liquid. Therefore, an interrelationship can be established between the work required to bring the molecule to the interface (γ) and the dielectric constant of the medium (or n_D^2). For our liquids, a good correlation was found with the Papazian equation (eq. 18). Table 7 lists the corresponding parameters.

Table 6
Estimated critical temperatures (T_c) and pressures (p_c) of the compounds studied [a].

	PC-SAFT EoS (eq. 1–5)		Joback method [b]		Guggenheim (eq. 16)	Eötvos (eq. 17)
Compound	T_c/K	p_c/MPa	T_c/K	p_c/MPa	T_c/K	T_c/K
Aa	679.14	4.14	725.76	3.93	790.62	733.58
L	656.64	2.97	697.57	2.58	670.97	643.63
Co	633.46	2.68	694.42	2.45	718.62	689.61
Ca	609.61	2.79	663.60	2.40	637.71	603.89
E	684.92	3.38	695.50	3.02	647.00	614.61

[a] Aa, anysil alcohol; L, linalool; Co, β-citronellol; Ca, citronellal; E, eucalyptol; [b] [39].

Table 7
Fit parameters of the surface tension correlations of the compounds studied [a]

	Papazian (eq. 18)			Pelofsky (eq. 19)			Murkerjee (eq. 20)		
	A	B	R^2	$\ln A_1$	B_1	R^2	$\ln A_2$	$B_2/3$	R^2
Aa	1026.3	−116.5	0.9993	3.800	−0.540	0.985	3.569	0.075	0.989
L	645.00	−89.74	0.9993	3.359	−0.312	0.985	3.128	0.097	0.974
Co	715.24	−99.92	0.9992	3.403	−0.536	0.969	3.136	0.089	0.991
Ca	707.12	−96.18	0.9997	3.549	−0.309	0.999	3.236	0.246	0.985
E	748.16	−106.1	0.9982	3.482	−0.400	0.995	3.139	0.188	0.989

[a] Aa, anysil alcohol; L, linalool; Co, β-citronellol; Ca, citronellal; E, eucalyptol.

4.2.6. Viscosity

The viscosity is the property that measures the resistance of a fluid to flow due to friction between its molecular layers. Usually, although kinematic viscosity is measured, the property that is tabulated is the dynamic one, which is related to it through density ($\eta = \rho\nu$). It depends on both molecular geometry and the strength of intermolecular interactions. In industry, less viscous solvents are preferred because they are easier to handle and more efficient in mass exchange processes. The liquids characterized were low-viscosity within the studied temperature range, with values below 22 mPa·s. Our data for L and E, were in agree with those of the literature with mean relative deviations lower than 5%. Figs. S3c and S4c display the graphical comparison. Both γ and η are largely a consequence of the strength of intermolecular forces. Therefore, it is to be expected that the more structured liquids will be the most viscous. In fact, the sequences obtained in this work for γ and η coincided. Table 7 lists the parameters of two equations that correlate both properties. The influence of temperature on the fluidity of liquids is more pronounced at lower temperatures, so the $\eta - T$ correlation is exponential (Fig. 3f). We used the VFT equation, whose expression and fitting parameters are given in Table 8. The A coefficient is the viscosity at 0 K; i.e., the contribution to the viscosity due to the geometry of the molecule. The B, and C, coefficients are related to the energy that must be overcome for the liquid to flow, the activation energy of viscous flow ($E_{a,\eta}$) calculated with the eq. 15. It decreased as T increased, as shown in Fig. 4 f.

Table 8
Correlation of the dynamic viscosity with temperature, VFT equation [a], of the compounds studied[b] . Fitting parameters (A, B, C) and mean relative deviations (MRD).

Compound	A	B	C	MRD/%
Aa	0.0619	635.11	181.94	0.310
L	0.0252	644.10	174.27	0.473
Co	0.0085	1247.39	119.00	0.437
Ca	0.0892	427.05	143.90	0.436
E	0.0372	797.14	109.80	0.155

[a] $\eta = A\exp\left[\frac{B}{T-C}\right]$; [b] Aa, anysil alcohol; L, linalool; Co, β-citronellol; Ca, citronellal; E, eucalyptol

4.3. Structure-property relationships

Table 9 lists several structural properties that can be related to the macroscopic properties studied in this work. The number of hydrogen bond donors (HBDs) and acceptors (HBAs) indicates the ability of the compounds to form hydrogen bonds. The topological polar surface area (TPSA) is calculated as the sum of surface contributions from polar functional groups. It is a measure of the polarity of the molecule, which is also highly correlated with HBs formation. Then, higher HBD, HBA, and TPSA values indicate higher possibility of interaction between molecules. The partition coefficient ($P_{0/w}$) indicates the affinity of a compound for a hydrophobic environment. A higher fraction of carbon sp^3 (Fsp^3) provides the molecule a more three-dimensional structure. Furthermore, the greater the number of rotatable bonds (Rot B), which is the number of single covalent bonds that allow free rotation, the greater the molecular flexibility. Table 9 also includes the calculated values of the molar refractivity from the structure as the sum of atom/bond contributions. With all of the above, a discussion of the results obtained from the measured properties as a function of the molecular structure of the compounds can be made.

In our phase change study (section 4.1), E and Aa were the only compounds for which melting and crystallization processes were detected. This is consistent with the known fact that crystal packing is favored in planar structures, i.e., those with lower Rot B. The ρ depends on both the strength of intermolecular interactions and molecular geometry. Anisyl alcohol has two acceptor sites and one donor site, the most polar surface, and one of the most rigid geometries. Its lower capacity for intermolecular interaction with neighboring hydrophobic regions appears to be negligible compared to the interactions established by HBs and dipole-dipole interactions. Both L and Co have one donor site and one acceptor site, a similar TPSA value, and flexible structures, with higher Fsp^3 and Rot B for Co. Finally, Ca and E have only one acceptor site, but E has the most rigid structure. Therefore, the density order found (Aa>E > L > Co > Ca) was consistent with the above, considering that the influence of geometry predominated for E. The R_m can be calculated with several software tools as the sum of

Table 9
Structural properties of the pure compounds from SwissADME platform [a]. Number of hydrogen bond donors (HBDs), number of hydrogen bond acceptors (HBAs), topological polar surface area (TPSA), logarithm of the partition coefficient $\log(P_{0/w})$, fraction of carbon sp^3 (Fsp^3), number of rotatable bonds (Rot B), and calculated molar refractivity $\left(R_m^{cal}\right)$ [b]

Chemical	HBDs	HBAs	TPSA/Å^2	$\log(P_{0/w})$	Fsp^3	Rot B	R_m^{cal}/(cm^3/mol)
Anisyl alcohol	1	2	29.46	1.40	0.25	2	39.06
Linalool	1	1	20.23	2.66	0.60	4	50.44
β-Citronellol	1	1	20.23	2.92	0.80	5	50.87
Citronellal	0	1	17.07	2.94	0.70	5	49.91
Eucalyptol	0	1	9.23	2.67	1	0	47.12

[a] Ref [50]; [b] Molar refractivity of the molecule in its standard state. It is calculated as sum of atom/bond contributions using OpenBabel Software.

atomic and bond contributions. Our values obtained from the experimental density and refractive index data matched with those listed in Table 9. The relative mean deviations ranged from 0.7% for Aa to 3.5% for E. The $C_{p,m}$ is greater the larger the M of the compound, and the greater the number HBs in the fluid because they consume energy. Both the presence of multiple bonds and the existence of rings affect the ability of normal vibrational modes to store energy. The L had a slightly higher $C_{p,m}$ value than Co, followed by Ca, Aa, and E. This sequence can be explained by the fact that L and Co have practically the same M and the same HBD and HBA, but L has a greater number of double bonds. Moreover, Ca and L has the same M and number of double bonds, but Ca is not HBA. The M of Aa is considerably lower than that the rest, but this can be compensated for by its greater capacity to form HBs, and the presence of the aromatic ring. The high interaction capacity of Aa and its rigidity, factors already discussed above, would explain the greater structuring of the fluid observed from the high values of its surface properties, γ and ΔH_s. Regarding η, both interactions and the molecular geometry of the liquid influence its value. In the case of interactions, the $E_{a,\eta}$ is the derived thermodynamic property related to them. Therefore, the sequence is expected to coincide with previous conclusions. In fact, Aa exhibited a significantly higher value than the other compounds, and Ca the lowest. Regarding geometry, Co exhibited greater steric hindrance than L due to its more three-dimensional structure, meaning a higher Fsp^3. This would explain the higher η of Co despite having a slightly lower $E_{a,\eta}$ value. The same occurs between E and Ca. A similar explanation can be given to justify the lower fluidity of E compared to Ca.

4.2. Modeling

In industrial chemical processes, it is necessary to establish optimal operating conditions to maximize efficiency while minimizing material and energy costs. The simulators used for this purpose must include thermodynamic tools that enable the estimation of the properties of the fluids involved, as determining these properties under any operating conditions is practically impossible. Different types of tools such as group contribution models, empirical correlations, models based on activity coefficients or excess energy, and equations of state have been developed. The latter are preferred because an excessively complex model can be difficult to implement and consume a significant amount of computation time. In addition, an inadequate model will yield erroneous results and therefore must be validated beforehand. Validating equations of state, such as the one used in this work (PC-SAFT) for pure compounds, will allow for the prediction of the thermodynamic behavior of the mixtures they comprise, and thus, the optimization of a large number of processes. In this EoS (section 3.1), compounds were described by 3 (Ca and E) or 5 (Aa, L, and Co) parameters depending on their auto-association capacity. They were calculated by minimizing deviations in vapor pressures (p_v) taken from the literature (where feasible) and from the densities measured in this work. For L and E [22,28], literature values of these parameters were found. Nevertheless, we have recalculated them for L to improve the results in the studied T range. A dispersion of points was observed in the literature p_v data. We choose those from Zaitsau et al. [24] to be included in the objective function along with our ρ values. For Co and Ca, we used p_v from Stejfa et al. [26] and Povh et al. [51], and ρ from this work. For Aa, no p_v data were found. The parameters obtained are summarized in Table 10, and a summary with the results of the modeling is found in Table 11. The calculated densities agreed with the experimental ones of this work, with mean relative deviations less than 0.45% in all compounds. For E, the deviation increases slightly in the literature data at pressures up to 60 MPa. Regarding $C_{p,m}$, the model also well predicted the thermal behavior, and the maximum deviation was obtained for L with a value of 4.1%. Fig. 5 shows the graphical comparison between our ρ and $C_{p,m}$ data, and those calculated with PC-SAFT EoS. As previously mentioned, knowing the critical point values of pure compounds is essential in the application of thermodynamic models used in the design of industrial operations. Values obtained from several correlations and methods were presented in section 4.2.5. They can be also estimated with the PC-SAFT EoS, and are listed in Table 6. The correct modeling of the volumetric and thermal behavior of these compounds with this EoS shown above could give reliability to these values.

5. Conclusion

Different substances commonly used as flavorings in the food and cosmetic industries were studied. They were anisyl alcohol (Aa), linalool (L), β-citronellol (Co), citronellal (Ca), and eucalyptol (E). Data of the density, speed of sound, refractive index, isobaric molar heat capacity, surface tension, and dynamic viscosity at 0.1 MPa, and up to 338.15 K were determined. From them, several properties as the isobaric expansivity, free intermolecular length, percentage of free volume, Joule-Thomson coefficient, critical point, and activation of viscous flow were estimated. In addition, the necessary parameters to be able to predict other thermodynamic properties of these pure compounds, and of their mixtures using the PC-SAFT EoS were obtained.

The Aa was the densest (even denser than water), most compact, and most viscous liquid. All results were consistent with expectations, considering the number of hydrogen bond donor and acceptor sites and the differences in geometries. The deviations obtained in the modeling

Table 10
Parameters of the pure compounds in the modeling with the PC-SAFT EoS. The type 2B (one donor and one acceptor site) was considered as association scheme for the compounds capable of self-association.

Compound	m	σ/ Å	ε/ K	$\kappa^{A_iB_i}$	$\varepsilon^{A_iB_i}$ / K
Anisyl alcohol [a]	7.065	2.880	213.0	0.09	2750
Linalool [a]	4.190	3.915	256.8	0.02	2100
β-citronellol [a]	6.453	3.359	197.0	0.09	2750
Citronellal [a]	4.210	3.850	244.6	–	–
Eucalyptol [b]	3.026	4.247	313.7	–	–

[a]This work; [b] [28].

Table 11
Results of the modeling with PC-SAFT EoS of the compounds studied. Temperature (T_{range}) and pressure (p_{range}) ranges, and mean relative deviations ($MRD(Y)^b$).

Compound	T_{range}/K	p_{range}/Pa	$MRD(p_v)^a$/%	$MRD(\rho)^a$/%	$MRD(C_{p,m})^a$/%
Anisyl alcohol	(278–338)	$0.1{\cdot}10^6$		0.44[b]	1.56[b]
	(303–313)	$0.1{\cdot}10^6$		0.34[c]	
Linalool	(278–338)	$0.1{\cdot}10^6$		0.09[b]	4.09[b]
	(284–353)	(6.4–1136)	0.58[d]		
	(283–333)	$0.1{\cdot}10^6$		0.22[e]	
	298	$0.1{\cdot}10^6$		0.19[f]	
	298	$0.1{\cdot}10^6$		0.09[g]	
	(283–328)	$0.1{\cdot}10^6$		0.29[h]	
	(406–462)	$(1.3–8){\cdot}10^4$	10.2[i]		
β-citronellol	(278–338)	$0.1{\cdot}10^6$		0.26[b]	3.32[b]
	(273–363)	(0.1–461)	6.59[j]		
	293	$0.1{\cdot}10^6$		0.14[k]	
Citronellal	(278–338)	$0.1{\cdot}10^6$		0.36[b]	0.99[b]
Eucalyptol	(278–338)	$0.1{\cdot}10^6$		0.17[b]	2.21[b]
	(293–323)	$0.1{\cdot}10^6$		0.20[l]	
	(278–298)	$0.1{\cdot}10^6$		0.19[m]	
	(278–358)	$(0.1–60){\cdot}10^6$		1.10[n]	
	(283–313)	$(0.1–20){\cdot}10^6$		0.68[o]	
	(293–344)	$0.1{\cdot}10^6$			1.72[p]
	(273–355)	$0.1{\cdot}10^6$			1.61[j]
	(278–323)	(71–1101)	2.11[q]	0.20[q]	
	(278–308)	(5.5–431)	12.21[j]		
	(283–313)	(8.3–592)	7.99[r]		

[a] $MRD(Y) = \frac{100}{n}\sum_{i=1}^{n}\left|\frac{Y_{i,PC-SAFT} - Y_{i,exp}}{Y_{i,exp}}\right|$; [b] This work; [c] [18]; [d] [24]; [e] [19]; [f] [20]; [g] [21]; [h] [22]; [i] [23]; [j] [26]; [k] [25]; [l] [27]; [m] [29]; [n] [28]; [o] [31]; [p] [32]; [q] [30]; [r] [33].

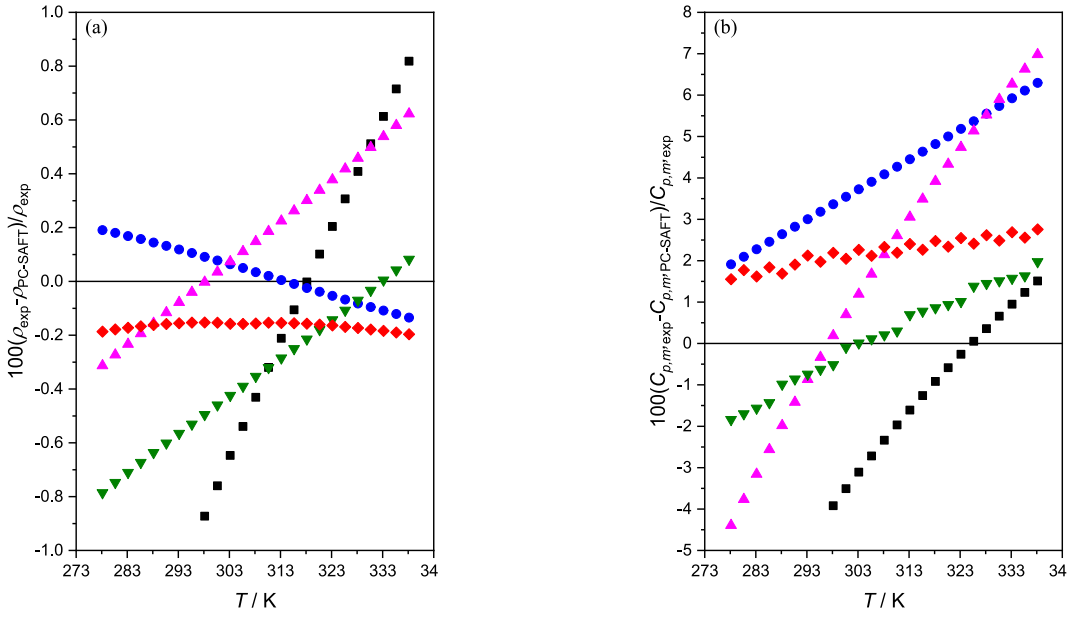

Fig. 5. Comparison between our experimental data and those predicted by PC-SAFT EoS. (a), Density (ρ); (b) isobaric molar heat capacity ($C_{p,m}$). (■), Anisyl alcohol; (●), Linalool; (▲), β-citronellol; (▼), citronellal; (◆), eucalyptol.

for ρ and $C_{p,m}$ were less than 1.10% and 4.1%, respectively.

CRediT authorship contribution statement

Roberto Martín-Ramo: Resources, Investigation, Data curation. **Candela Romero:** Methodology, Investigation, Data curation. **José Muñoz-Embid:** Validation, Supervision. **Héctor Artigas:** Validation, Formal analysis. **Carlos Lafuente:** Supervision, Project administration, Investigation. **Manuela Artal:** Writing – review & editing, Writing – original draft, Conceptualization.

Declaration of competing interest

The authors declare that they have no known competing financial interests or personal relationships that could have influenced the work reported in this paper.

Acknowledgments

PLATON research group acknowledges financial support from Gobierno de Aragón and Fondo Social Europeo "Construyendo Europa desde Aragón" _E31_23R.

Appendix A. Supplementary data

Supplementary data to this article can be found online at https://doi.org/10.1016/j.molliq.2026.129603.

Data availability

The authors confirm that the data supporting the findings of this study are available within the article and its supplementary materials.

References

[1] B. Pandit, P. Saha, Eco-friendly alternatives to conventional solvents: innovations and applications in pharmaceutical manufacturing, Sustainable Chemistry for Climate Action 7 (2025) 100140, https://doi.org/10.1016/j.scca.2025.100140.
[2] H. Sels, H. De Smet, J. Geuens, SUSSOL-using artificial intelligence for greener solvent selection and substitution, Molecules 25 (2020) 1–26, https://doi.org/10.3390/molecules25133037.
[3] L.J. Diorazio, D.R.J. Hose, N.K. Adlington, Toward a more holistic framework for solvent selection, Org. Process Res. Dev. 20 (2016) 760–773, https://doi.org/10.1021/acs.oprd.6b00015.
[4] G.A. Udourioh, B.M. Bazza, M.P. Pilani, M.M. Solomon, Therapeutic characteristics of essential oils: historical and scientific considerations, J. Appl. Sci. Environ. Manag. 29 (2025) 569–579, https://doi.org/10.4314/jasem.v29i2.28.
[5] J. Liang, Y. Zhang, P. Chi, H. Liu, Z. Jing, H. Cao, Y. Du, Y. Zhao, X. Qin, W. Zhang, D. Kong, Essential oils: chemical constituents, potential neuropharmacological effects and aromatherapy - a review, Pharmacological Research - Modern Chinese Medicine 6 (2023) 100210, https://doi.org/10.1016/j.prmcm.2022.100210.
[6] I. Montero-Fernández, N.C. Lobón, L.N. Gómez, J. Blanco-Salas, J.C.A. Gallego, Bioactive potential of terpenes from mediterranean scrub plants: a review, Molecules 30 (2025) 4268, https://doi.org/10.3390/molecules30214268.
[7] U. Yusupova, D. Tojiboeva, R. Mukhamatkhanova, D. Dusmatova, Essential oils as an alternative to synthetic antiseptics in cosmetics and personal care products, Chem. Biodivers. 23 (2026), https://doi.org/10.1002/cbdv.202503449.
[8] H. Pan, H. Li, S. Wu, C. Lai, D. Guo, De novo biosynthesis of anisyl alcohol and anisyl acetate in engineered escherichia coli, J. Agric. Food Chem. 71 (2023) 3398–3402, https://doi.org/10.1021/acs.jafc.2c08859.
[9] A.M. Api, A. Bartlett, D. Belsito, D. Botelho, M. Bruze, A. Bryant-Friedrich, G. A. Burton, M.A. Cancellieri, H. Chon, M. Cronin, S. Crotty, M.L. Dagli, W. Dekant, C. Deodhar, K. Farrell, A.D. Fryer, L. Jones, K. Joshi, A. Lapczynski, D.L. Laskin, M. Lavelle, I. Lee, H. Moustakas, J. Muldoon, T.M. Penning, A.H. Piersma, G. Ritacco, N. Sadekar, I. Schember, T.W. Schultz, F. Siddiqi, I.G. Sipes, G. Sullivan, Y. Thakkar, Update to RIFM fragrance ingredient safety assessment, anisyl alcohol, CAS registry number 105-13-5, Food Chem. Toxicol. 210 (2026) 115951, https://doi.org/10.1016/j.fct.2026.115951.
[10] Q. An, J.-N. Ren, X. Li, G. Fan, S.-S. Qu, Y. Song, Y. Li, S.-Y. Pan, Recent updates on bioactive properties of linalool, Food Funct. 12 (2021) 10370–10389, https://doi.org/10.1039/D1FO02120F.
[11] L.J. Marnett, S.M. Cohen, S. Fukushima, N.J. Gooderham, S.S. Hecht, I.M.C. M. Rietjens, R.L. Smith, T.B. Adams, M. Bastaki, C.L. Harman, M.M. McGowen, S. V. Taylor, GRASr2 evaluation of aliphatic acyclic and alicyclic terpenoid tertiary alcohols and structurally related substances used as flavoring ingredients, J. Food Sci. 79 (2014), https://doi.org/10.1111/1750-3841.12407.
[12] S.M. Cohen, G. Eisenbrand, S. Fukushima, N.J. Gooderham, F.P. Guengerich, S. S. Hecht, I. Rietjens, T. Rosol, C. Harman, S.V. Taylor, GRAS 29 flavoring substances, Food Technol. 74 (2020) 44–65.
[13] P.L. Santos, J.P.S.C.F. Matos, L. Picot, J.R.G.S. Almeida, J.S.S. Quintans, L. J. Quintans-Júnior, Citronellol, a monoterpene alcohol with promising pharmacological activities - a systematic review, Food Chem. Toxicol. 123 (2019) 459–469, https://doi.org/10.1016/j.fct.2018.11.030.
[14] P.L. Santos, R.G. Brito, M.A. Oliveira, J.S.S. Quintans, A.G. Guimarães, M.R. V. Santos, P.P. Menezes, M.R. Serafini, I.R.A. Menezes, H.D.M. Coutinho, A.A. S. Araújo, L.J. Quintans-Júnior, Docking, characterization and investigation of β-cyclodextrin complexed with citronellal, a monoterpene present in the essential oil of cymbopogon species, as an anti-hyperalgesic agent in chronic muscle pain model, Phytomedicine 23 (2016) 948–957, https://doi.org/10.1016/j.phymed.2016.06.007.
[15] T.J. Rosol, S.M. Cohen, G. Eisenbrand, S. Fukushima, N.J. Gooderham, F. P. Guengerich, S.S. Hecht, I.M.C.M. Rietjens, J.M. Davidsen, C.L. Harman, S. Kelly, D. Ramanan, S.V. Taylor, FEMA GRAS assessment of natural flavor complexes: lemongrass oil, chamomile oils, citronella oil and related flavoring ingredients, Food Chem. Toxicol. 175 (2023) 113697, https://doi.org/10.1016/j.fct.2023.113697.
[16] R.A. El Shiekh, A.M. Atwa, A.M. Elgindy, A.M. Mustafa, M.M. Senna, M. A. Alkabbani, K.M. Ibrahim, Therapeutic applications of eucalyptus essential oils, Inflammopharmacology 33 (2025) 163–182, https://doi.org/10.1007/s10787-024-01588-8.
[17] J.F. Campos, M.-C. Scherrmann, S. Berteina-Raboin, Eucalyptol: a new solvent for the synthesis of heterocycles containing oxygen, sulfur and nitrogen, Green Chem. 21 (2019) 1531–1539, https://doi.org/10.1039/C8GC04016H.
[18] A. Shakila, R. Raju, T. Srinivasa Krishna, R. Dey, V. Pandiyan, Molecular interaction studies in binary mixtures of tetrahydrofuran with arene-substituted alcohols: acoustic and volumetric study, Phys. Chem. Liquids 58 (2020) 263–279, https://doi.org/10.1080/00319104.2018.1564752.
[19] R.A. Clará, A.C.G. Marigliano, H.N. Sólimo, Density, viscosity, and refractive index in the range (283.15 to 353.15) k and vapor pressure of α-pinene, d-limonene, (±)-linalool, and citral over the pressure range 1.0 kPa atmospheric pressure, J. Chem. Eng. Data 54 (2009) 1087–1090, https://doi.org/10.1021/je8007414.
[20] P.M. Florido, I.M.G. Andrade, M.C. Capellini, F.H. Carvalho, K.K. Aracava, C. C. Koshima, C.E.C. Rodrigues, C.B. Gonçalves, Viscosities and densities of systems involved in the deterpenation of essential oils by liquid-liquid extraction: new UNIFAC-VISCO parameters, J. Chem. Thermodyn. 72 (2014) 152–160, https://doi.org/10.1016/j.jct.2013.11.026.
[21] R. Francesconi, C. Castellari, F. Comelli, Densities, viscosities, refractive indices, and excess molar enthalpies of methyl tert-butyl ether + components of pine resins and essential oils at 298.15 k, J. Chem. Eng. Data 46 (2001) 1520–1525, https://doi.org/10.1021/je010167n.
[22] M. Torcal, M.I. Teruel, J. García, J.S. Urieta, A.M. Mainar, P p t measurements of the (ethanol + linalool), (propan-1-ol + linalool), and (propan-2-ol + linalool) mixtures: cubic and statistical associating fluid theory-based equation of state analyses, J. Chem. Eng. Data 55 (2010) 5332–5339, https://doi.org/10.1021/je100581m.
[23] S.M. García-Abarrio, L. Haya, J.I. Pardo, J.S. Urieta, A.M. Mainar, Isobaric VLE of the mixture {(±)-linalool + ethanol}: a case study for the distillation of absolute and volatile oils, Journal of Chemical Thermodynamics 64 (2013) 182–186, https://doi.org/10.1016/j.jct.2013.05.022.
[24] D.H. Zaitsau, S.P. Verevkin, A.Y. Sazonova, Vapor pressures and vaporization enthalpies of 5-nonanone, linalool and 6-methyl-5-hepten-2-one, Data evaluation, Fluid Phase Equilib. 386 (2015) 140–148, https://doi.org/10.1016/j.fluid.2014.11.026.
[25] H. Li, Y. Han, C. Huang, C. Yang, (liquid + liquid) equilibria for (water + 1-propanol or acetone + β-citronellol) at different temperatures, J. Chem. Thermodyn. 86 (2015) 20–26, https://doi.org/10.1016/j.jct.2015.02.013.
[26] V. Štejfa, F. Dergal, I. Mokbel, M. Fulem, J. Jose, K. Růžička, Vapor pressures and thermophysical properties of selected monoterpenoids, Fluid Phase Equilib. 406 (2015) 124–133, https://doi.org/10.1016/j.fluid.2015.07.031.
[27] M. Almasi, R.S. Neyband, Exploring Structure–Property Relationships in Eucalyptol and 1-Alkanol Mixtures: A DFT and Experimental Study, Int. J. Thermophys. 45 (2024). doi:https://doi.org/10.1007/s10765-024-03414-3.
[28] S. Aparicio, R. Alcalde, M.J. Dávila, B. García, J.M. Leal, Properties of 1,8-cineole: a thermophysical and theoretical study, J. Phys. Chem. B 111 (2007) 3167–3177, https://doi.org/10.1021/jp067405b.
[29] P.A. Barata, M.L. Serrano, Densities and Viscosities of Thymol + 1,8-Cineole. https://pubs.acs.org/sharingguidelines, 1994.
[30] B. Gimeno, S. Martinez, A.M. Mainar, J.S. Urieta, P. Perez, Thermodynamic Behavior of (2-Propanol + 1,8-Cineole) Mixtures: Isothermal Vapor–Liquid Equilibria, Densities, Enthalpies of Mixing, and Modeling, Int. J. Mol. Sci. 24 (2023), https://doi.org/10.3390/ijms241210380.
[31] J.M. Lasarte, L. Martín, E. Langa, J.S. Urieta, A.M. Mainar, Setup and validation of a PρT measuring device. Volumetric behavior of the mixture 1,8-cineole + ethanol, J. Chem. Eng. Data 53 (2008) 1393–1400, https://doi.org/10.1021/je800024u.
[32] J.F. Martínez-López, S. Schneider, D. Salavera, A.M. Mainar, J.S. Urieta, J.I. Pardo, Molar heat capacities of the mixture {1,8-cineole + ethanol} at several temperatures and atmospheric pressure, J. Chem. Thermodyn. 92 (2016) 146–151, https://doi.org/10.1016/j.jct.2015.09.012.
[33] T. Guetachew, I. Mokbel, I. Batiu, Z. Cisse, J. Jose, Vapor pressures and sublimation pressures of eight constituents of essential oils at pressures in the range from 0.3 to 83,000 pa, ELDATA int, Electron. J. Phys. Chem. Dat. 5 (1999) 43–53.
[34] N. López, I. Delso, D. Matute, C. Lafuente, M. Artal, Characterization of xylitol or citric acid: choline chloride: water mixtures: structure, thermophysical properties, and quercetin solubility, Food Chem. 306 (2020), https://doi.org/10.1016/j.foodchem.2019.125610.
[35] V. Antón, J. Muñoz-Embid, I. Gascón, M. Artal, C. Lafuente, Thermophysical characterization of furfuryl esters: experimental and modeling, Energy Fuels 31 (2017), https://doi.org/10.1021/acs.energyfuels.7b00304.
[36] J. Gross, G. Sadowski, Perturbed-chain SAFT: An equation of state based on a perturbation theory for chain molecules, Ind. Eng. Chem. Res. 40 (2001) 1244–1260, https://doi.org/10.1021/ie0003887.
[37] J. Gross, G. Sadowski, Application of the perturbed-chain SAFT equation of state to associating systems, Ind. Eng. Chem. Res. 41 (2002) 5510–5515, https://doi.org/10.1021/ie010954d.
[38] B. Jacobson, Ultrasonic velocity in liquids and liquid mixtures, J. Chem. Phys. 20 (2004) 927–928, https://doi.org/10.1063/1.1700615.
[39] K.G. Joback, R.C. Reid, Estimation of pure-component properties from group-contributions, Chem. Eng. Commun. 57 (1987) 233–243, https://doi.org/10.1080/00986448708960487.
[40] E.A. Guggenheim, The principle of corresponding states, J. Phys. Chem. 13 (1945) 253–261.
[41] J.L.L. Shereshefsky, Surface tension of saturated vapors and the equation of eötvos, J. Phys. Chem. 35 (1930) 1712–1720, https://doi.org/10.1021/j150324a014.

[42] H.A. Papazian, Correlation of surface tension between various liquids, J. Am. Chem. Soc. 93 (1971) 5634–5636, https://doi.org/10.1021/ja00751a008.
[43] A.H. Pelofsky, Surface tension-viscosity relation for liquids, J. Chem. Eng. Data 11 (1966) 394–397, https://doi.org/10.1021/je60030a031.
[44] A. Gomes, L. Serrano, F. Farelo, Solid-Liquid Equilibria in 1,8-Clneole/Terpenic Hydrocarbon Systems. https://pubs.acs.org/sharingguidelines, 1988.
[45] PubChem, Database (2026). https://pubchem.ncbi.nlm.nih.gov/.
[46] The Food Database, Www.FooDB.Ca (n.d.).
[47] P.J. Linstrom, W.G. Mallard, NIST Chemistry Webbok, NIST Standard Reference Database Number 69, Gaithersburg MD, 20899, 2020, https://doi.org/10.18434/T4D303.
[48] V. Štejfa, M. Fulem, K. Růžička, C. Červinka, Thermodynamic study of selected monoterpenes III, J. Chem. Thermodyn. 79 (2014) 280–289, https://doi.org/10.1016/j.jct.2014.04.022.
[49] C. Zhou, X. Zhang, M. Qi, W. Zhao, S. Xiang, Evaluation and modification of group contribution methods for critical properties of organic compounds, Fluid Phase Equilib. 579 (2024), https://doi.org/10.1016/j.fluid.2023.114023.
[50] A. Daina, O. Michielin, V. Zoete, SwissADME: a free web tool to evaluate pharmacokinetics, drug-likeness and medicinal chemistry friendliness of small molecules, Sci. Rep. 7 (2017) 42717, https://doi.org/10.1038/srep42717.
[51] F.P. Povh, V.M. Rodrigues, M.A.A. Meireles, N. Pinheiro, Determinação da pressão de vapor de compostos orgânicos por cromatografia gasosa, Cienc. Tecnol. Aliment. 26 (2006) 465–474, https://doi.org/10.1590/S0101-20612006000200034.